How to cite: *Angew. Chem. Int. Ed.* **2022**, *61*, e202113340
International Edition: doi.org/10.1002/anie.202113340
German Edition: doi.org/10.1002/ange.202113340

Nitrogen Fixation | Hot Paper

Rhenium-Mediated Conversion of Dinitrogen and Nitric Oxide to Nitrous Oxide

Lukas Alig, Kim A. Eisenlohr, Yaroslava Zelenkova, Sven Rosendahl, Regine Herbst-Irmer, Serhiy Demeshko, Max C. Holthausen, and Sven Schneider**

Dedicated to Professor Holger Braunschweig on the occasion of his 60th birthday

Abstract: *Reductive splitting of N_2 is an attractive strategy towards nitrogen fixation beyond ammonia at ambient conditions. However, the resulting nitride complexes often suffer from thermodynamic overstabilization hampering functionalization. Furthermore, oxidative nitrogen atom transfer of N_2 derived nitrides remains unknown. We here report a Re^{IV} pincer platform that mediates N_2 splitting upon chemical reduction or electrolysis with unprecedented yield. The N_2 derived Re^{V} nitrides undergo facile nitrogen atom transfer to nitric oxide, giving nitrous oxide nearly quantitatively. Experimental and computational results indicate that outer-sphere ReN/NO radical coupling is facilitated by the activation of the nitride via initial coordination of NO.*

Haber–Bosch related hydrocarbon steam reforming accounts for a substantial share of the global energy consumption and anthropogenic CO_2 footprint.[1] N_2 fixation strategies for high- and mid-valent nitrogenous products without initial, energy demanding over-reduction are therefore highly attractive, but largely unexplored.[2] For example, redox economic biological and plasma processes towards nitrous oxide have been extensively examined,[3] but industrial production still relies on controlled NH_4NO_3 decomposition.[4] A thermochemically viable alternative could be the comproportionation of N_2 with nitric oxide [Eq. (1)],[5] but the demanding cleavage of the strong N_2 triple bond requires efficient catalysis.

$$N_2 + 2\,NO \rightarrow 2\,N_2O \quad \Delta_r H^0 = -3.9\,\text{kcal mol}^{-1} \tag{1}$$

In recent years, thermally, electro-, and photochemically driven N_2 splitting into nitride complexes has been advanced as an entry to N_2 fixation beyond ammonia.[6] Synthetic strategies typically relied on nucleophilic nitride reactivity and, so far, enabled catalytic formation of silyl- and borylamines.[6a,7] However, direct oxidative functionalization of nitrides that originate from N_2 is unknown. Cummins and co-workers demonstrated facile N_2O splitting into nitride and NO complexes at ambient temperatures (Scheme 1).[8] Later, the groups of Mayer and Caulton reported the reverse reaction, i.e., the release of N_2O by coupling of NO with terminal Os^{VI} and Ru^{IV} nitride complexes, respectively.[9] Motivated by this precedence, we here disclose the generation of N_2O from dinitrogen via electrochemical N_2 splitting and subsequent nitride transfer to NO at ambient conditions (Scheme 1).

Our group has previously explored reductive N_2 splitting by rhenium complexes with aliphatic pincer ligands into nucleophilic, terminal Re^{V} nitrides.[10] As the N-terminus defines the electrophilic site of nitric oxide,[11] a related platform was chosen to evaluate nitride/NO coupling. To avoid undesired pincer oxidation,[12] we resorted to the robust diphenylamido ligand $N(C_6H_3\text{-}4\text{-}CH_3\text{-}P^iPr_2)_2^-$ (PNP^-). Ison and co-workers recently reported the synthesis of the Re^{V} nitride [Re(N)Cl(PNP)] (**1**), yet not by N_2 activation.[13]

Heating $[ReCl_3(PPh_3)_2(MeCN)]$ and *H*PNP in benzene gives the Re^{IV} amide complex $[ReCl_3(PNP)]$ (**2**) in 86 %

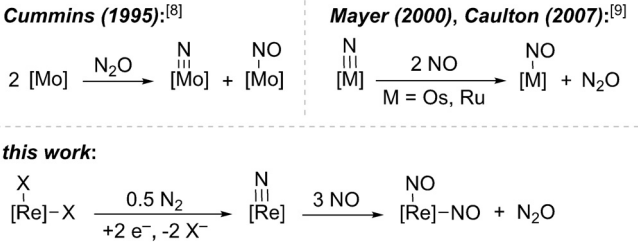

Scheme 1. Top: Nitrous oxide activation and generation reactions via triple bond metathesis reported in the literature. Bottom: Schematic reaction sequence for N_2O generation from N_2 and NO described here.

[*] L. Alig, Y. Zelenkova, S. Rosendahl, Dr. R. Herbst-Irmer, Dr. S. Demeshko, Prof. Dr. S. Schneider
Georg-August-Universität Göttingen
Institut für Anorganische Chemie
Tammannstrasse 4, 37077 Göttingen (Germany)
E-mail: sven.schneider@chemie.uni-goettingen.de
K. A. Eisenlohr, Prof. Dr. M. C. Holthausen
Goethe-Universität Frankfurt
Institut für Anorganische und Analytische Chemie
Max-von-Laue-Straße 7, 60438 Frankfurt am Main (Germany)
E-mail: max.holthausen@chemie.uni-frankfurt.de
Supporting information and the ORCID identification number(s) for the author(s) of this article can be found under: https://doi.org/10.1002/anie.202113340.

isolated yield.[14] Amide formation is supported by IR spectroscopy, while metal oxidation is attributed to H_2 evolution, as confirmed by gas chromatography. N–H bond weakening in related pincer ligands by metal coordination is well established.[15] The solution magnetic moment of **2** at room temperature ($\mu_{eff} = 1.63 \pm 0.1\ \mu_B$) supports low-spin Re^{IV}. While an EPR signal could not be resolved at temperatures down to 5 K, the well resolved ^{1}H NMR spectrum is in agreement with C_2 symmetry that arises from an axially chiral pincer ligand.[16] Single-crystal X-ray diffraction confirmed a planar amide group with a short N–Re bond (1.994(3) Å) that indicates π-bonding as origin for the low-spin configuration.[14]

Cyclic voltammetry (CV) under Ar shows two reductions of **2** as a reversible ($E_1^0 = -0.95$ V; all potentials vs. $Fc^{+/0}$) and an irreversible feature ($E_{2,pc} = -2.40$ V; $v = 100\ mV\,s^{-1}$), respectively (Scheme 2).[14] The low $Re^{III/II}$ potential is required for nitrogen activation as shown by chemical reduction with Na/Hg (2.5 equiv.) under N_2 (Scheme 2), which led to **1** in 60 % isolated yield. Reductive N_2 splitting was confirmed by isotopic labelling using ^{15}N NMR ($\delta =$ 363 ppm) and IR spectroscopy ($\nu(Re{\equiv}^{14}N) = 1080\ cm^{-1}$; $\nu(Re{\equiv}^{15}N) = 1047\ cm^{-1}$). The molecular structure of **1** in the crystal (Scheme 2)[14] showed distorted square-pyramidal coordination ($\tau_5 = 0.36$) with a Re≡N bond length (1.645(6) Å) that is in the typical range of Re^V nitride complexes.[10c,12,17] **1** was alternatively synthesized by in situ reduction of **2** with $CoCp_2$ and subsequent reaction with Me_3SiN_3.[14]

The reversibility of E_1 suggests that the unfavorably negative $Re^{III/II}$ couple E_2 results from slow Cl^- loss after reduction. We therefore moved to iodide as a better leaving group. [ReI_3(PNP)] (**3**) is easily prepared from **2** by halide metathesis. As hoped for, the first reduction of **3** under Ar ($E_{1,pc} = -0.79$ V; $v = 100\ mV\,s^{-1}$) becomes irreversible at scan rates up to $10\ V\,s^{-1}$ (Scheme 2), and a particularly large anodic shift with respect to **2** is obtained for the irreversible $Re^{III/II}$ wave ($E_{2,pc} = -1.69$ V; $v = 100\ mV\,s^{-1}$). In consequence, the N_2 splitting product [Re(N)I(PNP)] (**4**; Scheme 2) can be obtained with the mild reductant $CoCp_2$ (82 %) or by controlled potential electrolysis (CPE) in 1,2-difluorobenzene ($E_{appl.} = -1.67$ V), with unprecedented near quantitative yield (94 %) and Faradaic efficiency (98 %).[10c–e]

Benzene solutions of **1** or **4** slowly react with nitric oxide (1 atm) at room temperature over the course of minutes (Scheme 3 A). Nitrous oxide formation was confirmed and quantified by IR spectroscopy (2219 cm^{-1}), which is nearly quantitative in case of **1** (93.8 ± 4.3 %). With ^{15}N nitride labelled **^{15}N-1**, $^{15}N^{14}NO$ was obtained as the only isotopomer and isotopologue by ^{15}N NMR (Scheme 3 C), supporting N_2O release via selective nitride coupling with NO. Accordingly, the paramagnetic $\{Re(NO)_2\}^7$ dinitrosyl complex [ReCl-$(NO)_2$(PNP)] (**5**) could be isolated in 88 % yield from the reaction of **1** with nitric oxide. The magnetic susceptibility ($\mu_{eff} = 1.69 \pm 0.1\ \mu_B$) and X-band EPR signal ($g_{iso} = 2.01$) of **5** in CH_2Cl_2 at room temperature are in agreement with a low-spin ground state. The characteristic EPR line shape results from comparatively small, partially resolved $^{185/187}$Re hyperfine interaction (HFI, $A_{iso} = 140$ MHz), which is indicative of significant spin delocalization to the nitrosyl ligands.[18] This was confirmed by DFT calculations, which locate over 99 % of the excess spin density on the nitrosyl ligands with satisfyingly reproduced g-value ($g_{iso}^{DFT} = 2.03$) and $^{185/187}$Re HFI ($A_{iso}^{DFT} =$ 191 MHz).

Single-crystal X-ray diffraction confirmed the chemical composition of **5** (Scheme 3 B). While crystallographic disorder in space group $P2/n$ prevented an unequivocal determination of the configuration,[19] this was obtained by refinement in space group Pn and confirmed by vibrational spectroscopy. However, the disorder does not allow for detailed discussion of NO bonding. Three intense IR bands are observed in the characteristic region of NO stretching vibrations, both in solution and in the solid state ($\nu =$ 1694, 1634, 1597 cm^{-1}; Scheme 3 D).[20] Assignment to NO stretching modes was assisted by reaction of **1** with ^{15}NO, which leads to a bathochromic shift of only two bands in **^{15}NO-5** ($\nu_{15NO} =$ 1660 and 1599 cm^{-1}). The observation of two strong NO bands supports a *cis*-dinitrosyl configuration, as only one strong IR-active NO stretching vibration is expected for the *trans*-isomer. DFT calculations support this interpretation, placing the *cis*-isomer of **5** energetically below the *trans*-configuration by $\Delta^0G = 18\ kcal\,mol^{-1}$. Monitoring the reaction of **1** with NO by NMR (−20 °C) and IR (−15 °C) spectroscopies showed slow, clean conversion to **5** over the course of some hours. Besides the dinitrosyl product, small amounts of diamagnetic $\{Re(NO)_2\}^8$ complex [$Re(NO)_2$-(PNP)] (**6**) could be identified as side product by comparison with an authentic sample.

The mechanism was further probed by reacting **1** with NO in CH_2Cl_2/CCl_4 (4:1) to trap possible low-valent, coordinatively unsaturated rhenium intermediates via chlorine atom transfer.[9a] From this experiment, the mononitrosyl complex

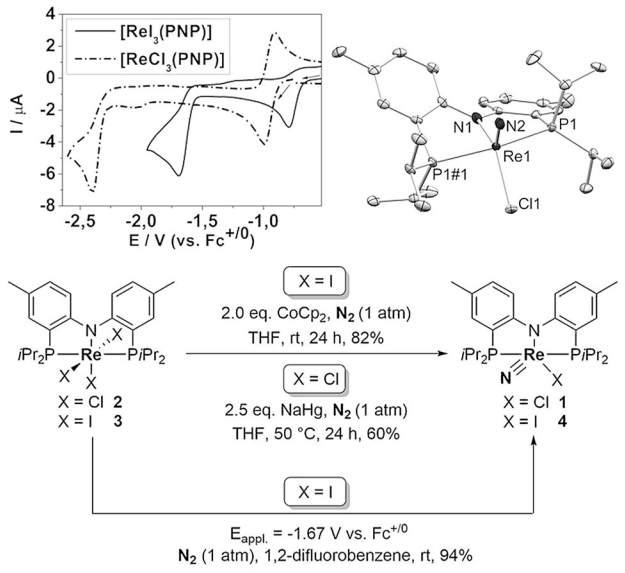

Scheme 2. Top left: CVs of **2** and **3** under Ar in THF. Top right: Molecular structure of **1** from single-crystal X-ray diffraction; ellipsoids are set at 50% probability; hydrogen atoms are omitted for clarity. Selected bond lengths [Å] and angles [°]: Re1–N2 1.645(6), Re1–N1 2.071(4), Re1–Cl1 2.3987(17), Re1–P1 2.4152(11), Re1–P1#1 2.4121-(11); N1-Re1-Cl1 132.09(5), P1-Re1-P1 153.73(3), N2-Re1-N1 116.7(2). Bottom: Reductive N_2 splitting.

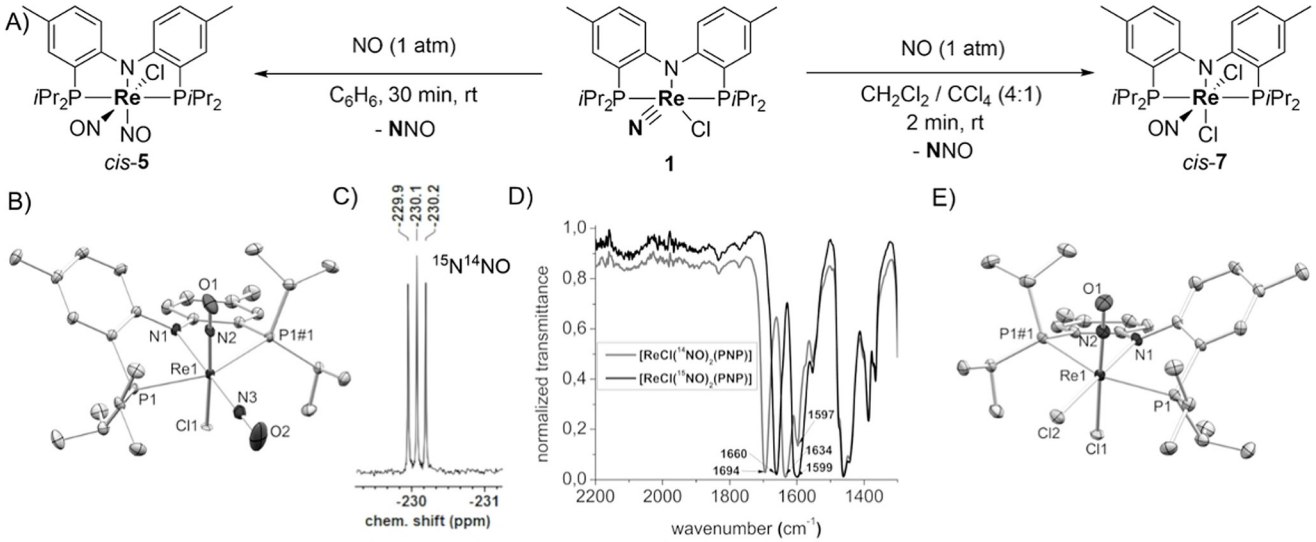

Scheme 3. A) Reaction of **1** with NO in benzene and CH_2Cl_2/CCl_4. B) Molecular structure of **5** with ellipsoids set at 50% probability; hydrogen atoms are omitted for clarity. Selected bond lengths [Å] and angles [°]: Re1–N1: 2.096(2), Re1–N2: 1.835(5), Re1–N3: 1.811(7), Re1–Cl1: 2.3635(18), Re1–Cl2: 2.378(4), Re1–P1: 2.4411(7), O1–N2: 1.215(6), O2–N3: 1.153(12); Re1-N3-O2: 180.0, P1-Re1-P1#1: 155.50(3), O1-N2-Re1: 177.0(5), N1-Re1-N3: 180.0. C) $^{15}N\{^1H\}$ NMR spectrum of ^{15}NNO in CD_2Cl_2 from the reaction of **^{15}N-1** with NO. D) Normalized transmittance ATR-IR spectra of **5** and **^{15}NO-5**. E) Molecular structure of **7** with ellipsoids set at 50% probability; hydrogen atoms are omitted for clarity. Selected bond lengths [Å] and angles [°]: Re1–N2: 1.810(6), N2–O1: 1.178(6), Re1–N1: 2.050(3), Re1–Cl1: 2.358(2), Re1–Cl2: 2.3943(9); Re1-N2-O1: 178.2(5), N1-Re1-N2: 91.17(19), P1-Re1-P1#1: 157.17(3), N1-Re1-Cl2: 180.0.

$[ReCl_2(NO)(PNP)]$ (**7**) was obtained in 84% yield (Scheme 3A). Concomitant formation of $^{15}N^{14}NO$ from **^{15}N-1** was verified by $^{15}N\{^1H\}$ NMR spectroscopy. X-ray crystallography confirmed the *cis*-dichloride configuration of $\{ReNO\}^5$ complex **7** (Scheme 3E) with a linearly coordinated nitrosyl ligand (Re-N-O: 178.2(5)°). SQUID magnetometric and X-band EPR spectroscopic characterization support an $S = 1/2$ ground state. However, the considerably larger $^{185/187}$Re HFI ($A_{iso} = 782$ MHz) as compared to **5**, suggests negligible spin delocalization to the nitrosyl ligand. This interpretation is supported by DFT computations, which place the SOMO of **7** orthogonal to the Re-NO axis.

The formation of **7** in the presence of CCl_4 suggests that the five-coordinate species [ReCl(NO)(PNP)] might be an intermediate in the reaction. We turned to DFT computations to evaluate electronic prerequisites for the formation of this species from **1**.[14] Direct attack of NO at the nitride atom in **1** gives a highly endergonic intermediate ($\Delta^0G = +25$ kcal mol^{-1}) with a prohibitively high reaction barrier ($\Delta^{\ddagger}G =$ 30 kcal mol^{-1}, Scheme S2). Instead, initial coordination of NO to the metal ion leads to nitrosyl nitride complex **D8** in an essentially thermoneutral and kinetically undemanding step (Figure 1A). The computed Re-N-O bond angle of **D8** (160.7°) is a structural manifestation of NO-centered radical character. NO coordination induces significant spin polarization (0.26α spin at $N_{nitride}$ and 0.24β spin at Re). Furthermore, natural bond orbital (NBO) analysis reveals concomitant weakening of the Re≡N interaction as expressed by the Wiberg bond index (WBI), which reduces from 2.55 (**1**) to 2.31 (**D8**, Figure 1B).

Subsequently, a second NO molecule can directly add to the nitride ligand via **TS2** with significantly reduced kinetic barrier ($\Delta^{\ddagger}G = 23$ kcal mol^{-1}). Singlet **TS2** exists only within the broken spin symmetry framework ($\langle S^2 \rangle = 0.79$) and affords the initial formation of a covalent σ bond by spin pairing of the singly occupied π* orbital of NO (β orbital in Figure 1C) and the in-plane non-bonding π* orbital (α orbital, WBI N-N in **TS2**: 0.53). Hence, mixing of the d_{xy} and Re≡N π* orbitals with the π* orbitals of the initially coordinating NO results in a singly occupied molecular orbital (SOMO) with significant nitride contribution (Figure 2), rendering N-N coupling via radical recombination more efficient than via a nucleophilic pathway.

NBO analysis of the resulting closed-shell intermediate **S9** reveals formation of an N≡NO triple bond and, in turn, substantial electron transfer to the metal ion, which is stabilized by increased Re→NO π backbonding within the $\{ReNO\}^6$ core. Coordination of the first NO ligand thus mediates electronic reorganization associated with Re≡N to N≡NO bond transformation. As a consequence, nitrous oxide is only weakly bonded to the Re ion. Release of N_2O and subsequent NO addition gives *cis*-**5** in two barrierless steps (Figure 1). The overall reaction from **1** to *cis*-**5** is strongly exergonic by −51 kcal mol^{-1}. The lowest computed path in Figure 1 emphasizes the role of initial NO binding for the activation of **1**. However, further mechanistic analysis will be required to account, e.g., for the formation of **6**.

In conclusion, rhenium mediated nitrogen atom transfer from dinitrogen to nitric oxide was described. Reductive N_2 activation with Re^{IV} trihalides $[ReX_3(PNP)]$ (X = Cl, I) gives the respective Re^{V} nitride complexes. More favorable iodide dissociation kinetics enable electrochemically driven N_2 splitting at relatively mild potential with unprecedented yields. The nitride products react with NO at ambient conditions to release near quantitative amounts of N_2O. Isotopic labelling confirmed nitride transfer over nitride

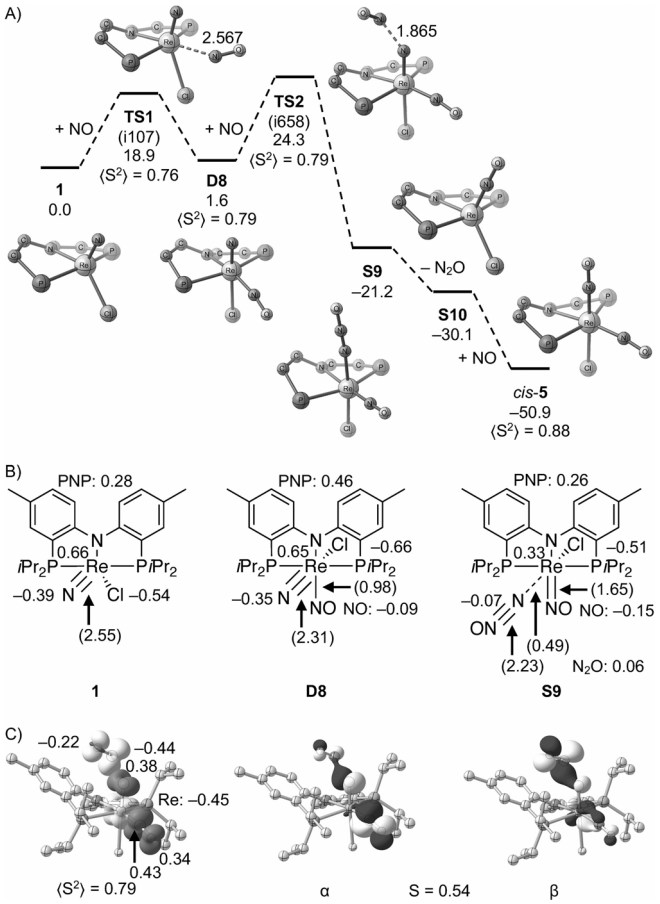

Figure 1. A) Lowest energy reaction pathway computed for the reaction of **1** with NO; alternative but less favorable pathways are presented in the Electronic Supporting Information (Δ^0G values in kcal mol^{-1} and selected bond lengths in Å; only truncated PNP ligands shown for clarity; S = singlet, D = doublet, TS = transition state). B) Selected NPA atomic charges and Wiberg bond indices (in parentheses) for **1**, **D8**, and **S9**. C) Spin density plot (isosurface at ± 0.005 a_0^{-3}) with natural spin populations for selected atoms and magnetic corresponding orbitals of **TS2** with spatial overlap S (isosurfaces at ± 0.05 $a_0^{-2/3}$, hydrogen atoms omitted for clarity).

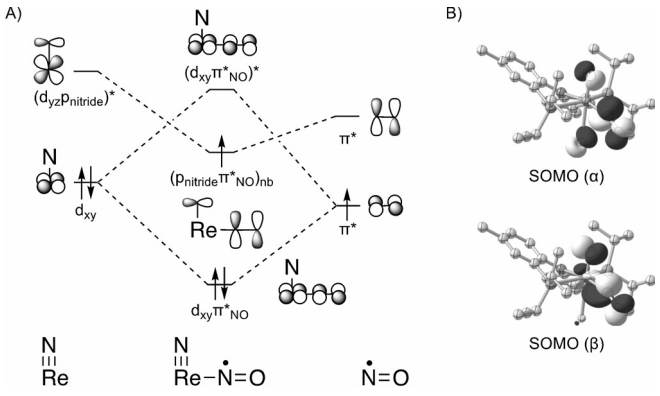

Figure 2. A) Qualitative MO diagram illustrating the mixing of selected MOs of **1** with the π* orbitals of NO. B) SOMO of **D8** (isosurfaces at ± 0.05 $a_0^{-2/3}$). Hydrogen atoms omitted for clarity.

oxygenation as the preferred pathway. Computational analysis indicates that direct N≡NO triple bond formation by NO attack at nitride **1** is not kinetically facile. Instead, initial coordination of NO spin polarizes the strong Re≡N bond and makes it more susceptible to radical N-N coupling. Importantly, our results offer a new strategy towards oxidative nitrogen fixation at ambient conditions via N_2 splitting into nitride complexes, which are otherwise notorious for thermodynamic overstabilization.

Acknowledgements

We are grateful to the European Research Council (ERC CoG 646747) for financial support. Quantum-chemical calculations were performed at the Center for Scientific Computing (CSC) Frankfurt on the Goethe and Fuchs high-performance compute clusters. Dr. A. C. Stückl is acknowledged for EPR measurements and Dr. S. J. K. Forrest for helpful discussions. Open Access funding enabled and organized by Projekt DEAL.

Conflict of Interest

The authors declare no conflict of interest.

Keywords: nitric oxide · nitride · nitrogen fixation · nitrous oxide · rhenium

[1] C. Smith, A. K. Hill, L. Torrente-Murciano, *Energy Environ. Sci.* **2020**, *13*, 331 – 344.
[2] J. G. Chen, R. M. Crooks, L. C. Seefeldt, K. L. Bren, R. M. Bullock, M. Y. Darensbourg, P. L. Holland, B. Hoffman, M. J. Janik, A. K. Jones, M. G. Kanatzidis, P. King, K. M. Lancaster, S. V. Lymar, P. Pfromm, W. F. Schneider, R. R. Schrock, *Science* **2018**, *360*, eaar6611.
[3] a) C. Ferousi, S. H. Majer, I. M. DiMucci, K. M. Lancaster, *Chem. Rev.* **2020**, *120*, 5252 – 5307; b) C. Douat, S. Hübner, R. Engeln, J. Benedikt, *Plasma Sources Sci. Technol.* **2016**, *25*, 025027.
[4] V. N. Parmon, G. I. Panov, A. Uriate, A. S. Noskov, *Catal. Today* **2005**, *100*, 115 – 131.
[5] M. W. Chase, Jr., *J. Phys. Chem. Ref. Data* **1998**, *9*, 1 – 1951.
[6] a) S. Kim, F. Loose, P. J. Chirik, *Chem. Rev.* **2020**, *120*, 5637 – 5681; b) S. J. K. Forrest, B. Schluschaß, E. Y. Yuzik-Klimova, S. Schneider, *Chem. Rev.* **2021**, *121*, 6522 – 6587; c) B. Schluschaß, J.-H. Borter, S. Rupp, S. Demeshko, C. Herwig, C. Limberg, N. Maciulis, J. Schneider, C. Würtele, V. Krewald, D. Schwarzer, S. Schneider, *JACS Au* **2021**, *1*, 879 – 894; d) J. Song, Q. Liao, X. Hong, L. Jin, N. Mézailles, *Angew. Chem. Int. Ed.* **2021**, *60*, 12242 – 12247; *Angew. Chem.* **2021**, *133*, 12350 – 12355.
[7] S. Bennaamane, M. F. Espada, A. Mulas, T. Personeni, N. Saffon-Merceron, M. Fustier-Boutignon, C. Bucher, N. Mézailles, *Angew. Chem. Int. Ed.* **2021**, *60*, 20210 – 20214; *Angew. Chem.* **2021**, *133*, 20372 – 20376.
[8] a) C. E. Laplaza, A. L. Odom, W. M. Davis, C. C. Cummins, *J. Am. Chem. Soc.* **1995**, *117*, 4999 – 5000; b) K. Severin, *Chem. Soc. Rev.* **2015**, *44*, 6375 – 6386.
[9] a) M. R. McCarthy, T. J. Crevier, B. Bennett, A. Dehestani, J. M. Mayer, *J. Am. Chem. Soc.* **2000**, *122*, 12391 – 12392; b) A. Walstrom, M. Pink, H. Fan, J. Tomaszewski, K. G. Caulton, *Inorg. Chem.* **2007**, *46*, 7704 – 7706.

[10] a) I. Klopsch, M. Finger, C. Würtele, B. Milde, D. B. Werz, S. Schneider, *J. Am. Chem. Soc.* **2014**, *136*, 6881 – 6883; b) I. Klopsch, M. Kinauer, M. Finger, C. Würtele, S. Schneider, *Angew. Chem. Int. Ed.* **2016**, *55*, 4786 – 4789; *Angew. Chem.* **2016**, *128*, 4864 – 4867; c) B. M. Lindley, R. S. van Alten, M. Finger, F. Schendzielorz, C. Würtele, A. J. M. Miller, I. Siewert, S. Schneider, *J. Am. Chem. Soc.* **2018**, *140*, 7922 – 7935; d) F. Schendzielorz, M. Finger, J. Abbenseth, C. Würtele, V. Krewald, S. Schneider, *Angew. Chem. Int. Ed.* **2019**, *58*, 830 – 834; *Angew. Chem.* **2019**, *131*, 840 – 844; e) R. S. van Alten, F. Wätjen, S. Demeshko, A. J. M. Miller, C. Würtele, I. Siewert, S. Schneider, *Eur. J. Inorg. Chem.* **2020**, 1402 – 1410.

[11] J. Hartung, *Chem. Rev.* **2009**, *109*, 4500 – 4517.

[12] G. P. Connor, B. Q. Mercado, H. M. C. Lant, J. M. Mayer, P. L. Holland, *Inorg. Chem.* **2019**, *58*, 10791 – 10801.

[13] N. S. Lambic, R. D. Sommer, E. A. Ison, *Dalton Trans.* **2018**, *47*, 758 – 768.

[14] See Electronic Supporting Information for experimental, spectroscopic, electrochemical, crystallographic and computational details. Deposition Numbers 2109793, 2109794, 2109795, 2109796, 2109797, 2109798, and 2109799 contain the supplementary crystallographic data for this paper. These data are provided free of charge by the joint Cambridge Crystallographic Data Centre and Fachinformationszentrum Karlsruhe Access Structures service www.ccdc.cam.ac.uk/structures. The ωB97X-D/def2-TZVPP level of DFT employed has been carefully validated against high-level CCSD(T*)-F12 results, cf. Section 2.2.2 in the Supporting Information.

[15] a) B. J. Charette, J. W. Ziller, A. F. Heyduk, *Inorg. Chem.* **2021**, *60*, 1579 – 1589; b) B. J. Charette, J. W. Ziller, A. F. Heyduk, *Inorg. Chem.* **2021**, *60*, 5367 – 5375.

[16] a) A. J. Kosanovich, W.-C. Shih, R. Ramírez-Contreras, O. V. Ozerov, *Dalton Trans.* **2016**, *45*, 18532 – 18540; b) A. J. Kosanovich, W.-C. Shih, O. V. Ozerov, *J. Organomet. Chem.* **2019**, *897*, 1 – 6; c) A. T. Radosevich, J. G. Melnick, S. A. Stoian, D. Bacciu, C.-H. Chen, B. M. Foxman, O. V. Ozerov, D. G. Nocera, *Inorg. Chem.* **2009**, *48*, 9214 – 9221.

[17] Q. J. Bruch, G. P. Connor, C.-H. Chen, P. L. Holland, J. M. Mayer, F. Hasanayn, A. J. M. Miller, *J. Am. Chem. Soc.* **2019**, *141*, 20198 – 20208.

[18] a) A. Klein, C. Vogler, W. Kaim, *Organometallics* **1996**, *15*, 236 – 244; b) T. Scheiring, A. Klein, W. Kaim, *J. Chem. Soc. Perkin Trans. 2* **1997**, 2569 – 2571.

[19] Refinement in the centrosymmetric space group *P*2/*n* with a crystallographic two-fold axis along N1-Re1-N3-O2 resulted in statistically disordered NO and chloride ligands. Solution in the lower symmetry space group *Pn* suggests co-crystallization of *cis*-**5** with a minor amount of *cis*-[$ReCl_2$(NO)(PNP)].

[20] B. Machura, *Coord. Chem. Rev.* **2005**, *249*, 2277 – 2307.

Manuscript received: October 1, 2021
Accepted manuscript online: October 29, 2021
Version of record online: December 2, 2021